

# Linguistic Query-Guided Mask Generation for Referring Image Segmentation

Zhichao Wei<sup>1</sup>Xiaohao Chen<sup>1</sup>Mingqiang Chen<sup>1</sup>Siyu Zhu<sup>1\*</sup><sup>1</sup>Alibaba Group

## Abstract

Referring image segmentation aims to segment the image region of interest according to the given language expression, which is a typical multi-modal task. Existing methods either adopt the pixel classification-based or the learnable query-based framework for mask generation, both of which are insufficient to deal with various text-image pairs with a fix number of parametric prototypes. In this work, we propose an end-to-end framework built on transformer to perform Linguistic query-Guided mask generation, dubbed *LGFormer*. It views the linguistic features as query to generate a specialized prototype for arbitrary input image-text pair, thus generating more consistent segmentation results. Moreover, we design several cross-modal interaction modules (e.g., vision-language bidirectional attention module, VLBA) in both encoder and decoder to achieve better cross-modal alignment. Extensive experiments demonstrate that our *LGFormer* achieves a new state-of-the-art performance on *ReferIt*, *RefCOCO+*, and *RefCOCOg* by large margins.

## 1. Introduction

Referring image segmentation (RIS) aims to generate a segmentation mask for the target object corresponding to a given language expression. In contrast to traditional segmentation tasks [10, 11, 12, 26] which can only process a predefined set of categories, referring image segmentation is no longer limited to specific classes and has wider applications including human-robot interaction [34] and interactive photo editing [3].

Although recent methods have achieved remarkable performance in this area, referring image segmentation is still a challenging task. The first challenge is *the alignment of cross-modal features*. As vision and language modality naturally maintain different attributes, aligning pixel-level visual features to corresponding holistic linguistic features is difficult. Another challenge is *the variance of text-image pairs*. The same language expression associated with different images could yield completely different segmentation results, while different language expressions related to the

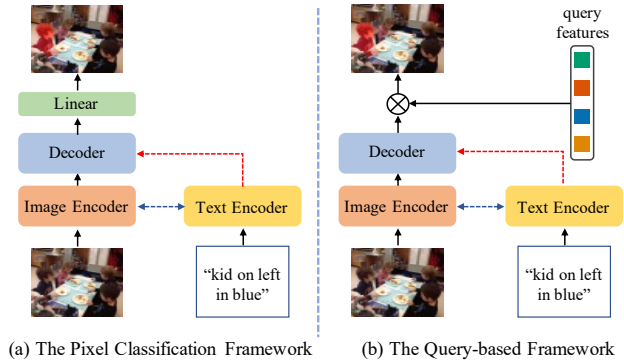


Figure 1. Illustration of the main architectures for referring image segmentation. (a) Pixel classification framework. (b) Query-based framework. Both [43] and our *LGFormer* belongs to the latter.

same image could produce the same segmentation results. Each text-image pair belongs to a unique class, making RIS an open-class segmentation task.

Most of the existing RIS methods are based on *pixel classification* framework, which uses a linear classifier to generate segmentation masks, as shown in Fig. 1(a). Previous methods [2, 8, 14, 15, 16, 40, 21, 23, 30, 36, 35, 24] often employ the decoder-fusion strategy, which first extracts visual and linguistic features from two independent uni-modal encoders respectively, then fuses these multi-modal representations into the same embedding space. In contrast, some recent works [9, 22, 38] adopt the encoder-fusion strategy, which performs cross-modal interactions in the early encoder stage. Although *pixel classification*-based methods have demonstrated their effectiveness, they mainly focus on resolving the issue of cross-modal features alignment but disregard the challenges that arise from the variance of text-image pairs in this task. From a prototype view, the pixel classification framework views the weights of the linear classifier as the prototype which groups pixels with high responses into segments [44]. However, one single fixed prototype is insufficient to describe the rich variance of text-image pairs. As shown in the first column of Fig. 2, these methods often fail to exploit the details (such as positions and attributes) and produce over- or under-segmented results with longer language expressions.

Recently, *query-based* methods [5, 6, 42] have greatly

\*Siyu Zhu is the corresponding author.

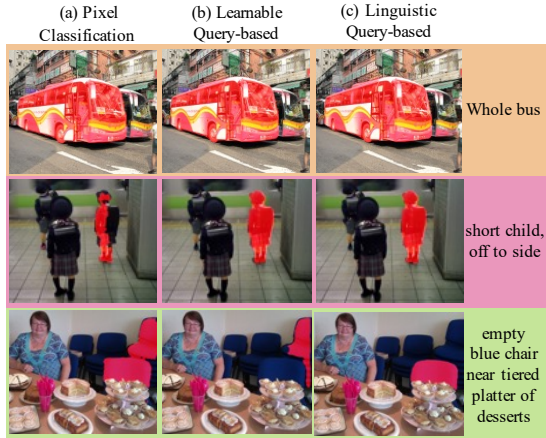


Figure 2. (a) The pixel classification-based methods perform well in easy cases but often produce inaccurate results with long language expressions. (b) The learnable query-based methods can capture more detailed information but still fail in extremely complicated language expression cases. (c) The linguistic query-based methods still generate high-quality segmentation results for both easy and complicated cases.

boosted the performance over the previous methods in the traditional image segmentation task. These methods introduce a fixed number of learnable queries as the input of the transformer decoder and associate each query with an instance. Based on this framework, the very recent work [43] achieved promising results on the RIS task, whose architecture is shown in Fig. 1(b). However, we argue that applying the learnable query-based framework to the RIS task directly is sub-optimal. Specifically, although the prototypes can be updated online with the multi-modal features, they are initialized with a set of fixed queries that are irrelevant to the input text-image pair, which greatly hinders the alignment with pixel embeddings and may generate inconsistent segmentation results. As is shown in the second column of Fig. 2, the learnable query-based method can capture some details with online updated prototypes and generate the more accurate results, but are still insufficient to deal with the complicated language expressions.

To extend this paradigm to the RIS task elegantly, we propose the notion of linguistic query and introduce LGFormer, an end-to-end framework for referring image segmentation. It utilizes the linguistic features as the query to generate a specialized prototype for the input text-image pair, which will group pixels with high responses into mask directly. Different from previous query-based segmentation methods, one query is enough in our LGFormer for the attendance of linguistic information. Moreover, to obtain more discriminative feature representations, we design a vision-language bidirectional attention (VLBA) module and a cross-modal decoder, performing cross-modal interactions at both the encoding and decoding stages.

To summarize, our main contributions are as follows:

- We introduce the linguistic query-guided mask generation mechanism to solve referring image segmentation for the first time. Given arbitrary text-image pair, we use the linguistic features as the query to generate a specialized prototype by interactions with visual features for mask generation.
- Based on the proposed mask generation mechanism, we design a simple yet effective framework, dubbed LGFormer. It use the specialized prototype to group image pixels with high responses into segmentation mask directly in an end-to-end manner. Moreover, we design several cross-modal interaction modules for better cross-modal alignment.
- The proposed method achieves state-of-the-art results on multiple datasets, including ReferIt[19], RefCOCO+ [41], and RefCOCOg [29], by large margins without bells and whistles.

## 2. Related Work

**Pixel Classification Framework.** Motivated by the success of *pixel classification* framework in traditional semantic segmentation, most of the existing methods adopt the FCN-like head to decode the mask. Early works mainly focused on fusing multi-modal representations on the decoder. Hu *et al.* [13] proposed to utilize CNN and RNN to extract visual and linguistic features separately and then obtain a segmentation mask through the concatenation-convolution operation. Based on this pipeline, some works [23, 2, 14, 39] improved the performance by utilizing more powerful feature encoders and designing more ingenious fusion strategies (*e.g.*, recurrent fusion). With the success of attention mechanisms in the communities of natural language processing and computer vision, follow-up works [40, 27, 8, 20] attempted to model intra-modal and cross-modal relationships by adopting self-attention and cross-attention operations. For example, Ye *et al.* [40] proposed Cross-Modal Self-Attention (CMSA) to highlight informative visual and linguistic elements. Ding *et al.* [8] used vision-guided attention to generate multiple linguistic queries which understand language expression from different aspects. Kim *et al.* [20] conducted both intra-modality and inter-modality interactions by self-attention operations, alleviating the weakness of CNN in capturing language information and cross-modal information. Recent studies [9, 18, 38] have shown that cross-modal interactions during feature extraction can further enhance multi-modal alignment. Feng *et al.* [9] replaced the vision encoder with a multi-modal encoder by adopting an early cross-modal interaction strategy, which achieved deep interweaving between visual and linguistic features. Yang *et al.* [38]

adopted language-aware visual attention during feature encoding and effectively exploited the transformer encoder for modeling multi-modal context. Instead of using a unimodal pre-trained backbone for features extraction, Wang *et al.* [35] transfers multi-modal knowledge of the contrastive language-image pretraining (CLIP) [31] for better cross-modal alignment.

**Query-based Framework.** Some recent image segmentation works [33, 6, 5, 42] employ transformers with additional cross-attention as mask decoder which generates segmentation masks by object queries (*i.e.*, learnable embeddings). Wang *et al.* [33] proposed an end-to-end panoptic segmentation method named Max-DeepLab which employs a mask decoder to generate dynamic filters. Cheng *et al.* [6] proposed MaskFormer which shows good performance in both semantic- and instance-level segmentation tasks in a unified manner. By using mask attention, multi-scale high-resolution features, and optimizing the training strategy, Mask2Former [5] outperformed specialized architectures across different segmentation tasks by a universal image segmentation architecture. From the perspective of clustering, Yu *et al.* [42] proposed kMax-DeepLab, endowing better interpretation ability of mask decoder. The very recent work CoupAlign [43] is also based on the query-based framework. However, this method introduces a set of (*i.e.*, 100) learnable queries to obtain mask proposals and generate masks by additional integration operations. We argue that adopting the learnable query for the RIS task is sub-optimal, as the learnable query is irrelevant to the input. To extend this query-based paradigm into referring image segmentation task, we propose to treat the vision-attended linguistic features as the unique query for generating a linguistic prototype to group pixels into segments.

### 3. Methodology

In this section, we first overview two frameworks used in existing methods from a prototype view, including the pixel classification framework and the query-based framework, and describe how we improve the latter to fit the referring image segmentation task. Then, we introduce the network structure and details of the proposed LGFormer.

#### 3.1. Linguistic Prototype

From a prototype view, the process of segmentation can be seen as utilizing the prototype  $\rho_k$  to group pixel embeddings  $E_i \in \mathbb{R}^D$  with high response and generate the mask[44], which can be formulated as follow:

$$p(k|E_i) = \frac{\exp(\rho_k^T E_i)}{\sum_{k'=1}^K \exp(\rho_{k'}^T E_i)} \quad (1)$$

where  $p(k|E_i)$  is the probability that  $i$ -th pixel being assigned to class  $k$ ,  $\rho_k$  is the prototype for  $k$ -th class and  $K$  is the number of classes for semantic segmentation.

**Pixel Classification Prototype.** Inspired by traditional semantic segmentation works[26, 4], prevalent RIS methods adopt the pixel classification framework to generate the segmentation mask. Specifically, these methods use a linear classifier, *i.e.*, a fully connected layer, to assign each pixel embedding  $E_i \in \mathbb{R}^D$  a semantic label:

$$p(k|E_i) = \frac{\exp(w_k^T E_i)}{\sum_{k'=1}^K \exp(w_{k'}^T E_i)} \quad (2)$$

where  $w_k$  is the learned weights for the  $k$ -th class in the linear classifier. According to Eq 1 and Eq 2, the pixel classification framework views the weights of the linear classifiers as the prototype. In the RIS task, the number of class  $K$  is 2 for only one foreground object needs to be segmented, which means this mechanism seeks to learn a global prototype for open-world text-image pairs and generates segmentation results by grouping pixels with high responses. We argue that this approach is insufficient for the RIS task since each input text-image pair belongs to a unique class, and using one global prototype to deal with infinite text-image instances is insufficient.

**Learnable Query-based Prototype.** Different from the pixel classification framework, the recent query-based framework generates segments by applying the online updateable prototypes to group pixel embeddings. In contrast to the pixel classification framework that uses a global prototype to fit various text-image pairs, the learnable query-based framework initializes  $K$  (*e.g.*, 100) learnable prototypes in the embedding space, and updates them with the multi-modal features for more accurate segmentation. This online updating process of  $\rho_k$  can be formulated as:

$$\rho_k = q_k + g(q_k, V, L) \quad (3)$$

where  $q_k$  is  $k$ -th learned queries,  $V$  is the visual input and  $L$  is the linguistic input.  $g(\cdot)$  represents cross-modal interactions that generate residuals to update prototypes towards a more proper position according to the input text-image pair. The semantic label of each pixel can be obtained by applying Eq. 1. Compared to a pixel classification-based framework that learns a fixed prototype, the prototypes in a query-based framework can be online updated by multi-modal features. But the prototype  $\rho_k$  is still constrained by the fixed learned query  $q_k$  and fails to represent the various text-image instances, especially when the language expression is complicated.

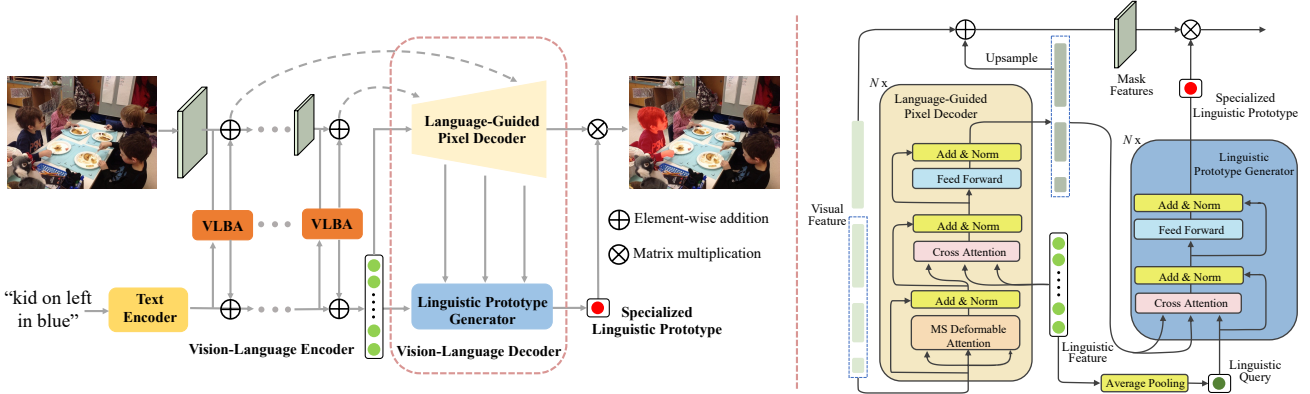


Figure 3. An overview of the LGFormer framework is shown on the left side of the figure. It consists of a vision-language encoder with our proposed VLBA module for cross-modal interactions, a vision-language decoder with a language-guided pixel decoder for integrating multi-scale visual features and linguistic features, and a linguistic prototype generator for generating the visual-attended linguistic prototypes. The more detailed design of the vision-language decoder is shown on the right side of the figure.

**Linguistic Prototype.** To deal with various text-image inputs, an intuitive idea is to increase the number of learnable prototypes discussed above. However, too many prototypes may confuse the model associating them with input instances, and make it difficult for the network to converge, as demonstrated in [1]. Here raises a natural question: *“Is there an efficient way to handle open-world text-image pairs with fewer queries?”*

This work answers this question by incorporating the linguistic features into the query vector to generate a linguistic prototype for each text-image instance. This specialized linguistic prototype is initialized by linguistic prior and then further updated with multi-modal information as follow:

$$\rho = f(L) + g(f(L), V, L) \quad (4)$$

where  $L$  is the input text and  $f(\cdot)$  represent a text encoder. As such, the specialized linguistic prototype can capture instance-level information of the input, thus achieving more accurate segmentation. The proposed mechanism can handle the arbitrary number of classes with only one non-parametric query vector conditioned on linguistic information, which can fit the RIS task with open class naturally.

### 3.2. Network Architecture

As illustrated in Fig. 3, the proposed LGFormer takes a text-image pair as input and outputs a segmentation mask for the region of interest. Firstly, the input image and text are transformed into multi-modal features, which leverage the proposed VLBA for early cross-modal fusion. Secondly, the multi-scale visual features and linguistic features are fed into the pixel decoder to generate fine-grained semantic representations. Then, the multi-scale visual features are sent to the linguistic prototype generator to update the linguistic query continuously. As such, the instance-level information of the input text-image pair can be captured by the linguistic query and it will act as the specialized

prototype for pixels grouping. Finally, the mask is obtained by the dot product between the linguistic prototype and the mask features refined by the pixel decoder.

#### 3.2.1 Vision-Language Encoder

**Vision Backbone.** For the input image, we adopt a deep hierarchical vision model (e.g., Swin Transformer [25]) to obtain multi-scale visual features maps with a resolution of 1/4, 1/8, 1/16, and 1/32 of the original spatial size. These feature maps contain rich details and semantics, which will facilitate better cross-modal alignment.

**Language Backbone.** For the input language expression with  $T$  words, we first use a tokenizer (e.g., BERT Tokenizer [7]) to transform them into a set of word embeddings, and then adopt a deep language model (e.g., BERT [7]) to generate linguistic features which will be used for every subsequent process in our model.

**Vision-Language Bidirectional Attention.** We propose a vision-language bidirectional attention module (VLBA) for early cross-modal alignment based on PWAM [38]. In contrast to PWAM which views linguistic information as supplementary, the proposed VLBA regards linguistic features as equally important as visual features. As shown in Fig. 4, the proposed VLBA takes the visual features  $V \in \mathbb{R}^{H \times W \times C_v}$  from the intermediate layer of visual backbone and the linguistic features  $L \in \mathbb{R}^{T \times C_l}$  from the last layer of linguistic backbone as inputs, where  $H, W, C_v, T$  and  $C_l$  are the height, width, channels of the visual feature maps, the word length and the channels of linguistic feature maps. And then update  $V$  and  $L$  as follow:

$$A = \frac{V_q L_k^T}{\sqrt{C_v}} \quad (5)$$

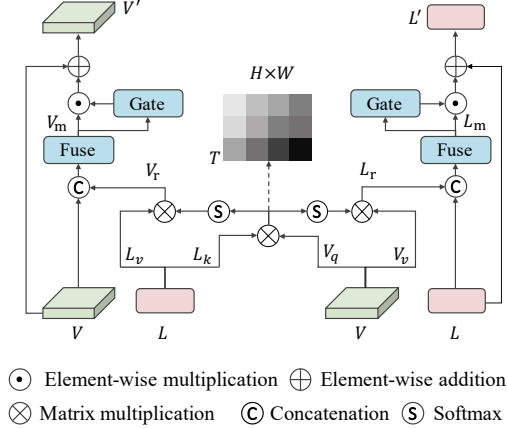


Figure 4. The detailed process of our proposed visual-language bidirectional attention (VLBA) module with a symmetric structure. The module takes linguistic features  $L$  and visual features  $V$  as input and updates them mutually.

$$V_r = w_1 (\text{softmax}(A) L_v) \quad (6)$$

$$L_r = w_2 (\text{softmax}(A^T) V_v) \quad (7)$$

where  $V_q$  and  $V_v$  are the query embeddings and value embeddings of  $V$ .  $L_k$  and  $L_v$  are the key embeddings and value embeddings of  $L$ .  $w_1$  and  $w_2$  represent linear projections.  $V_r$  and  $L_r$  are the responses for visual features and linguistic features, respectively.

$$V_m = \text{fuse}(\text{cat}(V, V_r)) \quad (8)$$

$$L_m = \text{fuse}(\text{cat}(L, L_r)) \quad (9)$$

$$V' = V + V_m \odot \text{gate}(V_m) \quad (10)$$

$$L' = L + L_m \odot \text{gate}(L_m) \quad (11)$$

where  $\odot$  denotes element-wise multiplication. Both the  $\text{fuse}(\cdot)$  and  $\text{gate}(\cdot)$  are implemented as a two-layer MLP.

### 3.2.2 Vision-Language Decoder

We design a cross-modal decoder to perform linguistic prototype-based decoding, which consists of four components: language-guided pixel decoder, vision-guided linguistic prototype generator, and prediction head.

**Language-Guided Pixel Decoder.** The pixel decoder is used to gradually recover the spatial resolution of visual features. To make per-pixel feature representations more discriminative for mask generation, we also incorporate the linguistic features in this process which will enhance instance features of interest and weaken irrelevant background features. As such, the uni-modal pixel decoder is converted into a cross-modal pixel decoder, performing spatial resolution recovery and multi-scale cross-modal fusion simultaneously.

As shown in Fig. 3 right, our pixel decoder consists of  $N$  transformer layers and a upsample layer for generating mask features. In each transformer layer, multi-scale deformable attention [45], cross attention [32], and feed-forward network are employed sequentially for feature refinement. Specifically, the transformer layers take the multi-scale visual feature maps with resolutions 1/8, 1/16, and 1/32 of original spatial size and linguistic features from the vision-language encoder as inputs, and outputs the refined multi-scale visual feature maps which have the same spatial resolutions as the inputs. After this multi-scale cross-modal features fusion, the bilinear interpolation is applied to the feature maps with a resolution 1/8 to obtain the mask features for mask generation.

**Linguistic Prototype Generator.** This generator is used to transform the sentence-level linguistic query to the specialized linguistic prototype for grouping the pixel embedding, which is implemented as a  $N$ -layer standard transformer decoder [32]. Through cross-modal interactions with visual features, the linguistic prototype is associated with the unique referred object, making it easier to handle arbitrary text-image pairs.

To generate the specialized prototype for the input text-image instance, we first obtain the sentence-level embedding of linguistic features by average pooling across word dimensions. Then, this sentence-level embedding together with the multi-scale visual features with resolution 1/32, 1/16, and 1/8 of the original image from the pixel decoder are fed into the linguistic prototype generator. We follow [5] to update the linguistic prototype with multi-scale visual features in a sequential manner.

**Prediction Head.** A lightweight head is built on top of the linguistic prototype generator to further transform the prototype. This head is implemented as a 3-layer MLP with ReLU activation except for the last layer. Given the specialized linguistic prototype and the mask features with a resolution 1/4 of the original spatial size from the pixel decoder, the segmentation mask is generated by their dot product.

### 3.3. Vision-Language Contrastive Learning

In contrast to existing pixel classification-based methods which perform feature alignment implicitly with classification loss, our linguistic prototype-based framework can easily introduce contrastive learning for explicit feature alignment, thus achieving better segmentation results.

Given the specialized linguistic prototype  $L_o \in \mathbb{R}^{C_o}$  and mask features  $V_o \in \mathbb{R}^{N_o \times C_o}$  from the decoder, the pixel-text contrastive loss is formulated as:

Method	Backbone	ReferIt	RefCOCO			RefCOCO+			RefCOCOg	
		test	val	testA	testB	val	testA	testB	val(U)	test(U)
BRINet [14]	ResNet-101	63.46	60.98	62.99	59.21	48.17	52.32	42.11	-	-
CMPC [15]	ResNet-101	65.53	61.36	64.53	59.64	49.56	53.44	43.23	-	-
LSCM [16]	ResNet-101	66.57	61.47	64.99	59.55	49.34	53.12	43.50	-	-
CMPC+ [24]	ResNet-101	-	62.47	65.08	60.82	50.25	54.04	43.47	-	-
MCN [28]	Darknet-53	-	62.44	64.20	59.71	50.62	54.99	44.69	49.22	49.40
EFN [9]	ResNet-101	66.70	62.76	65.69	59.67	51.50	55.24	43.01	-	-
BUSNet [37]	ResNet-101	-	63.27	66.41	61.39	51.76	56.87	44.13	-	-
CGAN [27]	ResNet-101	-	64.86	68.04	62.07	51.03	55.51	44.06	51.01	51.69
LTS [17]	DarkNet-53	-	65.43	67.76	63.08	54.21	58.32	48.02	54.40	54.25
VLT [8]	DarkNet-53	-	65.65	68.29	62.73	55.50	59.20	49.36	52.99	56.65
ReSTR [20]	ViT-B-16	70.18	67.22	69.30	64.45	55.78	60.44	48.27	54.48	-
CRIS [35]	ResNet-101	-	70.47	73.18	66.10	62.27	68.08	53.68	59.87	60.36
LAVT [38]	Swin-B	-	72.73	75.82	68.79	62.14	68.38	55.10	61.24	62.09
CoupAlign [43]	Swin-B	73.28	<b>74.70</b>	77.76	70.58	62.92	68.34	56.69	62.84	62.22
<b>LGFormer (ours)</b>	Swin-B	<b>75.80</b>	74.69	<b>77.81</b>	<b>70.66</b>	<b>65.69</b>	<b>71.53</b>	<b>57.89</b>	<b>63.72</b>	<b>65.18</b>

Table 1. Comparisons with state-of-the-art methods.

$$\mathcal{L}^i = \begin{cases} -\log \sigma((L_o \cdot V_o^i)) & \text{if } y^i = 1 \\ -\log(1 - \sigma((L_o \cdot V_o^i))) & \text{otherwise} \end{cases} \quad (12)$$

$$\mathcal{L} = \frac{1}{N_o} \sum_{i=1}^{N_o} \mathcal{L}^i(L_o, V_o^i) \quad (13)$$

where  $\sigma(\cdot)$  is the sigmoid function.  $N_o$  and  $C_o$  are the spatial size and channels of the visual feature maps  $V_o$ .  $y^i \in \{0, 1\}$  and  $V_o^i$  are the ground truth label and the per-pixel embeddings at the  $i$ -th position of  $V_o$ .

The contrastive loss pulls pixel embeddings in the region of interest to the linguistic prototype and pushes that of the background away from it.

## 4. Experiments

### 4.1. Datasets and Metrics

**Datasets.** We evaluate the proposed method on four commonly used datasets including ReferIt [19], RefCOCO [41], RefCOCO+ [41] and RefCOCOg [29]. ReferIt [19] contains 19,894 images with 130,525 language expressions that refer to 96,654 object regions. Language expressions in ReferIt are relatively shorter than the other datasets. RefCOCO [41] contains 19,994 images and 142,209 language expressions that refer to 50,000 segmented object regions. The average length of language expressions in this dataset is 3.5 words. RefCOCO+ [41] contains 26,711 images and 104,560 language expressions that refer to 54,822 segmented object regions. Especially, expressions in RefCOCO+ do not contain words describing the absolute locations of objects, which makes it more challenging than RefCOCO. RefCOCOg [29] consists of 104,560 expressions involving 54,822 objects in 26,711 images. In contrast to

the above three datasets, RefCOCOg has a longer average sentence length of 8.4 words, containing more words about the appearance and location of the referent.

**Metrics.** We adopt three metrics to evaluate the proposed methods including overall intersection-over-union (oIoU), mean intersection-over-union (mIoU), and  $Precision@X$ . The oIoU is defined as the ratio of the total intersection area over the total union area between the predictions and ground truth of all test data, which reflects the overall segmentation accuracy. The mIoU calculates the average IoU of all test data, which reflects the generalization ability of the model.  $Precision@X$  measures the percentage of test data that exceeds the predefined IoU threshold  $X$ , and in this paper  $X \in \{0.5, 0.7, 0.9\}$ .

### 4.2. Implementation Details.

We utilize PyTorch to implement our method. To make a fair comparison with the state-of-the-art methods, official pre-trained Swin-Transformer-Base [25] and BERT-Base-Uncased [7] models are adopted as the visual encoder and linguistic encoder respectively, and the other parameters in our model are initialized randomly. For network optimization, we adopt the AdamW optimizer with a weight decay of 0.01 and an initial learning rate of  $5e-5$  with the polynomial scheduler. The decoder layer number  $N$  is set to 6 by default. All input images are resized to  $480 \times 480$  and no data augmentation is applied. We train the model for 40 epochs, and the batch size is set to 32.

During inference, the predicted results with the spatial stride 4 are interpolated into the original spatial size and then binarized with the threshold of 0.5 as the final segmentation mask without any post-process.

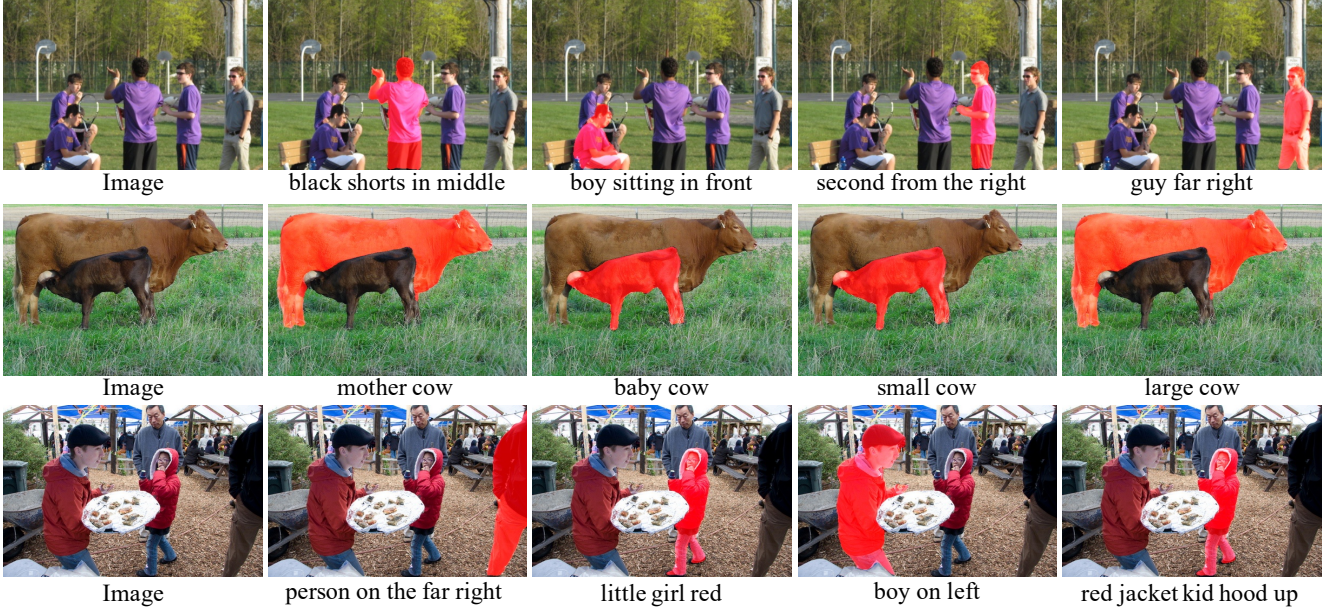


Figure 5. Visualization examples of LGFormer on the RefCOCO val set.

### 4.3. Comparisons with State-of-the-art

In Tab. 1, we compare our method with existing state-of-the-art methods on four widely used datasets detailed in Sec. 4.1. It can be seen that our LGFormer outperforms other methods on almost all datasets with large margins.

On ReferIt, LGFormer achieves the oIoU of 75.80% without bells and whistles, which is 2.52% higher than the previous state-of-the-art method CoupAlign [43]. Similarly, our method also achieves the best results on RefCOCOg and RefCOCO+. In particular, on the more complex and difficult RefCOCO+, LGFormer still achieves a oIoU gain of more than 1.2%, especially on the testA split, which is 3.19%. On RefCOCOg, another dataset with a longer average length of language expressions, our method also achieves notable oIoU improvements over other methods by 2.96% at most. These results show that the proposed linguistic query-based mechanism is able to capture instance-level information through cross-modal interactions, making it more flexible and effective in difficult cases. We visualize some segmentation results on the RefCOCO val subset in Fig. 5, where each image is associated with different language expressions. These visualization results further demonstrate the effectiveness of the proposed method in handling variations of images and language.

### 4.4. Ablation Study

In this section, we investigate the effect of the core components in our model. The more challenging val split with complex scenarios of RefCOCO+ [41] is adopted. Experimental settings are the same as Sec. 4.2.

Query Type	Num	P@0.5	P@0.7	P@0.9	oIoU	mIoU
Learnable	1	75.59	67.48	29.37	63.15	66.38
	10	77.37	69.64	31.96	64.26	68.14
Linguistic	1	<b>78.96</b>	<b>71.30</b>	<b>33.35</b>	<b>65.69</b>	<b>69.44</b>

Table 2. Ablation studies of query type.

**Linguistic Query vs. Learnable Query.** We study the effects of different query types on performance, including the proposed linguistic query and learnable queries, as shown in Tab. 2, where we use a 3-layer MLP to integrate the multiple masks when the learnable query number is 10. From the first two rows of Tab. 2, we can see that a larger query number is helpful to boost the performance for capturing more details of the input text-image pair. From the last row of Tab. 2, the proposed linguistic query-based mechanism surpasses the learnable queries-based counterparts by large margins, which shows that our approach can capture instance-level information of the input text-image pair for accurate mask generation.

In order to further analyze the ability of the linguistic query for the complicated expressions, we divide the RefCOCO+(val) into four parts according to the length of expressions  $l_{text}$  (the long expressions are usually more complicated than the short expressions) and evaluate the oIoU respectively. Specifically, we divide  $1 \leq l_{text} < 3$ ,  $3 \leq l_{text} < 8$ ,  $8 \leq l_{text} < 13$  and  $l_{text} \geq 13$  as *simple set*, *moderate set*, *complicated set*, and *extremely complicated set*. Tab. 3 shows that the linguistic query-based method outperforms the learnable query-based method by 0.6%, 1.3%, 2.5% and **7.7%** under the oIoU metric on the

Method	Length			
	[1,3)	[3,8)	[8,13)	[13,+∞)
Learnable	75.20	64.11	51.64	43.13
Linguistic	<b>75.86</b>	<b>65.33</b>	<b>54.61</b>	<b>50.81</b>

Table 3. Ablation studies of complicated expressions.

*simple set*, *moderate set*, *complicated set*, and *extremely complicated set* respectively. The superiority of the linguistic query-based method becomes more obvious as the linguistic complexity increases. We visualize some segmentation results of the cases with complicated language expressions in Fig. 6, the learnable query-based method is restricted by the query number and thus fails to fit open-world text-image pairs with diverse scenarios. In contrast, our linguistic prototype-based mechanism is able to capture the instance-level information of the input text-image instance, thus generating a more consistent mask even in complicated scenarios.

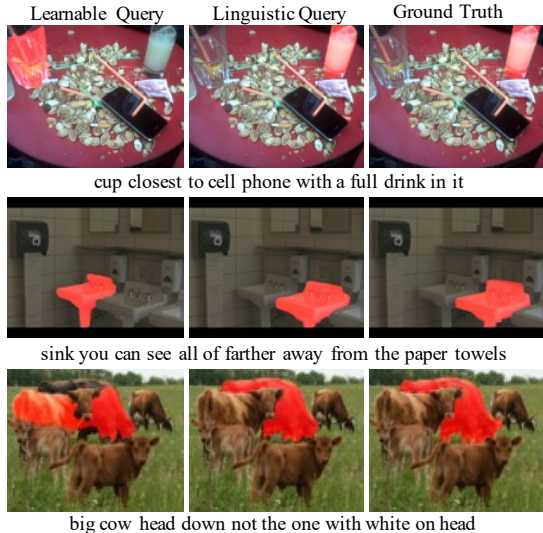


Figure 6. Visualization of the cases with complicated expressions.

**Cross-modal Fusion Modules.** Tab. 4 shows the effect of different cross-modal fusion modules on the performance, including vision-language bidirectional attention (VLBA) at the encoder, language-to-vision attention (L2VA) and vision-to-language attention (V2LA) at the decoder. The baseline (i.e., first row) is built by removing L2VA and V2LA and replacing the VLBA with PWAM proposed in [38]. It can be seen that our baseline has already achieved strong performance, exceeding other state-of-the-art methods with obvious margins. This is because our linguistic query-based mechanism is able to capture instance-level information from visual and linguistic inputs, thus promoting more consistent and accurate segmentation results.

From the second row of Tab. 4, the VLBA module brings 0.9% oIoU improvements. We can also see that cross-modal fusion modules L2VA and V2LA at the decoder further

VLBA	L2VA	V2LA	oIoU	mIoU
			63.91	67.47
✓			64.81	68.68
✓	✓		65.22	68.75
✓	✓	✓	<b>65.69</b>	<b>69.44</b>

Table 4. Ablation studies of cross-modal fusion modules.

Layer Num	oIoU	mIoU
3	65.31	69.02
6	<b>65.69</b>	<b>69.44</b>

Table 5. Ablation studies of decoder layer’s number.

Query of L2VA	oIoU	mIoU
sentence embeddings	65.36	68.93
word embeddings	<b>65.69</b>	<b>69.44</b>

Table 6. Ablation results on the input of pixel decoder.

boost the oIoU performance by 0.41% and 0.47% respectively. These results demonstrate that cross-modal interactions in both the encoder and decoder are essential for achieving better alignment.

**Number of Decoder Layers.** To investigate the effect of the number of decoder layers, we vary it to {3, 6}. Note that the layer numbers of L2VA and V2LA are kept the same in this study. As shown in Tab. 5, the model performance is enhanced consistently with more layers. We choose 6 as the default decoder layer number.

**Word Embeddings vs. Sentence Embeddings for L2VA.** For the L2VA in the language-guided pixel decoder, the linguistic features can be used in two forms, i.e., original word embeddings and sentence embeddings, where the sentence embeddings are generated by the average pooling across word dimensions. As shown in Tab. 6, using the word embeddings can outperform using sentence embeddings by 0.33% oIoU gain. This is because fine-grained linguistic features can promote better alignment than global features.

## 4.5. Conclusion

In this paper, we introduce the linguistic query-guided mask generation for referring image segmentation task for the first time, and propose an end-to-end framework LGFormer. It utilizes the linguistic features as the query to generate a specialized prototype and groups pixels with high responses into the segmentation mask directly. Moreover, we design several cross-modal fusion modules in both encoder and decoder to achieve better alignment, including the VLBA module in the encoder, language-to-vision attention (L2VA) and vision-to-language attention (V2LA) in the decoder. Extensive experiments demonstrate that our LGFormer surpasses previous state-of-the-art methods on multiple benchmark datasets by large margins.

## References

- [1] Nicolas Carion, Francisco Massa, Gabriel Synnaeve, Nicolas Usunier, Alexander Kirillov, and Sergey Zagoruyko. End-to-end object detection with transformers. In *European Conference on Computer Vision (ECCV)*, 2020. 4
- [2] Ding-Jie Chen, Songhao Jia, Yi-Chen Lo, Hwann-Tzong Chen, and Tyng-Luh Liu. See-through-text grouping for referring image segmentation. In *International Conference on Computer Vision (ICCV)*, 2019. 1, 2
- [3] Jianbo Chen, Yelong Shen, Jianfeng Gao, Jingjing Liu, and Xiaodong Liu. Language-based image editing with recurrent attentive models. In *Conference on Computer Vision and Pattern Recognition (CVPR)*, 2018. 1
- [4] Liang-Chieh Chen, George Papandreou, Iasonas Kokkinos, Kevin Murphy, and Alan L Yuille. Deeplab: Semantic image segmentation with deep convolutional nets, atrous convolution, and fully connected crfs. *IEEE transactions on pattern analysis and machine intelligence (PAMI)*, 2017. 3
- [5] Bowen Cheng, Ishan Misra, Alexander G Schwing, Alexander Kirillov, and Rohit Girdhar. Masked-attention mask transformer for universal image segmentation. In *Conference on Computer Vision and Pattern Recognition (CVPR)*, 2022. 1, 3, 5
- [6] Bowen Cheng, Alex Schwing, and Alexander Kirillov. Pixel classification is not all you need for semantic segmentation. *Advances in Neural Information Processing Systems (NIPS)*, 2021. 1, 3
- [7] Jacob Devlin, Ming-Wei Chang, Kenton Lee, and Kristina Toutanova. Bert: Pre-training of deep bidirectional transformers for language understanding. *arXiv preprint arXiv:1810.04805*, 2018. 4, 6
- [8] Henghui Ding, Chang Liu, Suchen Wang, and Xudong Jiang. Vision-language transformer and query generation for referring segmentation. In *International Conference on Computer Vision (ICCV)*, 2021. 1, 2, 6
- [9] Guang Feng, Zhiwei Hu, Lihe Zhang, and Huchuan Lu. Encoder fusion network with co-attention embedding for referring image segmentation. In *Conference on Computer Vision and Pattern Recognition (CVPR)*, 2021. 1, 2, 6
- [10] Jun Fu, Jing Liu, Haijie Tian, Yong Li, Yongjun Bao, Zhiwei Fang, and Hanqing Lu. Dual attention network for scene segmentation. In *Conference on Computer Vision and Pattern Recognition (CVPR)*, 2019. 1
- [11] Junjun He, Zhongying Deng, Lei Zhou, Yali Wang, and Yu Qiao. Adaptive pyramid context network for semantic segmentation. In *Conference on Computer Vision and Pattern Recognition (CVPR)*, 2019. 1
- [12] Kaiming He, Georgia Gkioxari, Piotr Dollár, and Ross Girshick. Mask r-cnn. In *International Conference on Computer Vision (ICCV)*, 2017. 1
- [13] Ronghang Hu, Marcus Rohrbach, and Trevor Darrell. Segmentation from natural language expressions. In *European Conference on Computer Vision (ECCV)*, 2016. 2
- [14] Zhiwei Hu, Guang Feng, Jiayu Sun, Lihe Zhang, and Huchuan Lu. Bi-directional relationship inferring network for referring image segmentation. In *Conference on Computer Vision and Pattern Recognition (CVPR)*, 2020. 1, 2, 6
- [15] Shaofei Huang, Tianrui Hui, Si Liu, Guanbin Li, Yunchao Wei, Jizhong Han, Luoqi Liu, and Bo Li. Referring image segmentation via cross-modal progressive comprehension. In *Conference on Computer Vision and Pattern Recognition (CVPR)*, 2020. 1, 6
- [16] Tianrui Hui, Si Liu, Shaofei Huang, Guanbin Li, Sansi Yu, Faxi Zhang, and Jizhong Han. Linguistic structure guided context modeling for referring image segmentation. In *European Conference on Computer Vision (ECCV)*, 2020. 1, 6
- [17] Ya Jing, Tao Kong, Wei Wang, Liang Wang, Lei Li, and Tieniu Tan. Locate then segment: A strong pipeline for referring image segmentation. In *Conference on Computer Vision and Pattern Recognition (CVPR)*, 2021. 6
- [18] Aishwarya Kamath, Mannat Singh, Yann LeCun, Gabriel Synnaeve, Ishan Misra, and Nicolas Carion. Mdetr-modulated detection for end-to-end multi-modal understanding. In *International Conference on Computer Vision (ICCV)*, 2021. 2
- [19] Sahar Kazemzadeh, Vicente Ordonez, Mark Matten, and Tamara Berg. Referitgame: Referring to objects in photographs of natural scenes. In *Conference on Empirical Methods in Natural Language Processing (EMNLP)*, 2014. 2, 6
- [20] Namyup Kim, Dongwon Kim, Cuiling Lan, Wenjun Zeng, and Suha Kwak. Restr: Convolution-free referring image segmentation using transformers. In *Conference on Computer Vision and Pattern Recognition (CVPR)*, 2022. 2, 6
- [21] Ruiyu Li, Kaican Li, Yi-Chun Kuo, Michelle Shu, Xiaojuan Qi, Xiaoyong Shen, and Jiaya Jia. Referring image segmentation via recurrent refinement networks. In *Conference on Computer Vision and Pattern Recognition (CVPR)*, 2018. 1
- [22] Zizhang Li, Mengmeng Wang, Jianbiao Mei, and Yong Liu. Mail: A unified mask-image-language trimodal network for referring image segmentation. *arXiv preprint arXiv:2111.10747*, 2021. 1
- [23] Chenxi Liu, Zhe Lin, Xiaohui Shen, Jimei Yang, Xin Lu, and Alan Yuille. Recurrent multimodal interaction for referring image segmentation. In *International Conference on Computer Vision (ICCV)*, 2017. 1, 2
- [24] Si Liu, Tianrui Hui, Shaofei Huang, Yunchao Wei, Bo Li, and Guanbin Li. Cross-modal progressive comprehension for referring segmentation. *Pattern Analysis and Machine Intelligence (PAMI)*, 2021. 1, 6
- [25] Ze Liu, Yutong Lin, Yue Cao, Han Hu, Yixuan Wei, Zheng Zhang, Stephen Lin, and Baining Guo. Swin transformer: Hierarchical vision transformer using shifted windows. In *International Conference on Computer Vision (ICCV)*, 2021. 4, 6
- [26] Jonathan Long, Evan Shelhamer, and Trevor Darrell. Fully convolutional networks for semantic segmentation. In *Conference on Computer Vision and Pattern Recognition (CVPR)*, 2015. 1, 3
- [27] Gen Luo, Yiyi Zhou, Rongrong Ji, Xiaoshuai Sun, Jinsong Su, Chia-Wen Lin, and Qi Tian. Cascade grouped attention

- network for referring expression segmentation. In *ACM International Conference on Multimedia (ACM MM)*, 2020. [2](#), [6](#)
- [28] Gen Luo, Yiyi Zhou, Xiaoshuai Sun, Liujuan Cao, Chenglin Wu, Cheng Deng, and Rongrong Ji. Multi-task collaborative network for joint referring expression comprehension and segmentation. In *Conference on Computer Vision and Pattern Recognition (CVPR)*, 2020. [6](#)
- [29] Junhua Mao, Jonathan Huang, Alexander Toshev, Oana Camburu, Alan L Yuille, and Kevin Murphy. Generation and comprehension of unambiguous object descriptions. In *Conference on Computer Vision and Pattern Recognition (CVPR)*, 2016. [2](#), [6](#)
- [30] Edgar Margffoy-Tuay, Juan C Pérez, Emilio Botero, and Pablo Arbeláez. Dynamic multimodal instance segmentation guided by natural language queries. In *European Conference on Computer Vision (ECCV)*, 2018. [1](#)
- [31] Alec Radford, Jong Wook Kim, Chris Hallacy, Aditya Ramesh, Gabriel Goh, Sandhini Agarwal, Girish Sastry, Amanda Askell, Pamela Mishkin, Jack Clark, et al. Learning transferable visual models from natural language supervision. In *International Conference on Machine Learning (ICML)*, 2021. [3](#)
- [32] Ashish Vaswani, Noam Shazeer, Niki Parmar, Jakob Uszkoreit, Llion Jones, Aidan N Gomez, Łukasz Kaiser, and Illia Polosukhin. Attention is all you need. *Advances in Neural Information Processing Systems (NIPS)*, 2017. [5](#)
- [33] Huiyu Wang, Yukun Zhu, Hartwig Adam, Alan Yuille, and Liang-Chieh Chen. Max-deeplab: End-to-end panoptic segmentation with mask transformers. In *Conference on Computer Vision and Pattern Recognition (CVPR)*, 2021. [3](#)
- [34] Xin Wang, Qiuyuan Huang, Asli Celikyilmaz, Jianfeng Gao, Dinghan Shen, Yuan-Fang Wang, William Yang Wang, and Lei Zhang. Reinforced cross-modal matching and self-supervised imitation learning for vision-language navigation. In *Conference on Computer Vision and Pattern Recognition (CVPR)*, 2019. [1](#)
- [35] Zhaoqing Wang, Yu Lu, Qiang Li, Xunqiang Tao, Yandong Guo, Mingming Gong, and Tongliang Liu. Cris: Clip-driven referring image segmentation. In *Conference on Computer Vision and Pattern Recognition (CVPR)*, 2022. [1](#), [3](#), [6](#)
- [36] Jianzong Wu, Xiangtai Li, Xia Li, Henghui Ding, Yunhai Tong, and Dacheng Tao. Towards robust referring image segmentation. *arXiv preprint arXiv:2209.09554*, 2022. [1](#)
- [37] Sibe Yang, Meng Xia, Guanbin Li, Hong-Yu Zhou, and Yizhou Yu. Bottom-up shift and reasoning for referring image segmentation. In *Conference on Computer Vision and Pattern Recognition (CVPR)*, 2021. [6](#)
- [38] Zhao Yang, Jiaqi Wang, Yansong Tang, Kai Chen, Hengshuang Zhao, and Philip HS Torr. Lavt: Language-aware vision transformer for referring image segmentation. In *Conference on Computer Vision and Pattern Recognition (CVPR)*, 2022. [1](#), [2](#), [4](#), [6](#), [8](#)
- [39] Linwei Ye, Zhi Liu, and Yang Wang. Dual convolutional lstm network for referring image segmentation. *IEEE Transactions on Multimedia*, 2020. [2](#)
- [40] Linwei Ye, Mrigank Rochan, Zhi Liu, and Yang Wang. Cross-modal self-attention network for referring image segmentation. In *Conference on Computer Vision and Pattern Recognition (CVPR)*, 2019. [1](#), [2](#)
- [41] Licheng Yu, Patrick Poirson, Shan Yang, Alexander C Berg, and Tamara L Berg. Modeling context in referring expressions. In *European Conference on Computer Vision (ECCV)*, 2016. [2](#), [6](#), [7](#)
- [42] Qihang Yu, Huiyu Wang, Siyuan Qiao, Maxwell Collins, Yukun Zhu, Hartwig Adam, Alan Yuille, and Liang-Chieh Chen. k-means mask transformer. In *European Conference on Computer Vision (ECCV)*, 2022. [1](#), [3](#)
- [43] Zicheng Zhang, Yi Zhu, Jianzhuang Liu, Xiaodan Liang, and Wei Ke. Coupalign: Coupling word-pixel with sentence-mask alignments for referring image segmentation. *arXiv preprint arXiv:2212.01769*, 2022. [1](#), [2](#), [3](#), [6](#), [7](#)
- [44] Tianfei Zhou, Wenguan Wang, Ender Konukoglu, and Luc Van Gool. Rethinking semantic segmentation: A prototype view. In *Conference on Computer Vision and Pattern Recognition (CVPR)*, 2022. [1](#), [3](#)
- [45] Xizhou Zhu, Weijie Su, Lewei Lu, Bin Li, Xiaogang Wang, and Jifeng Dai. Deformable detr: Deformable transformers for end-to-end object detection. *arXiv preprint arXiv:2010.04159*, 2020. [5](#)